

# Mechanism of the Stereoselective Alkyl Group Exchange between Alkylboranes and Alkylzinc Compounds. Quest for Novel Types of Boron–Metal Exchange Reactions

Eike Hupe,<sup>†</sup> Paul Knochel,<sup>†</sup> and Kálmán J. Szabó<sup>\*‡</sup>

Department of Chemistry, Ludwig-Maximilians-University Munich, Butenandtstrasse 5-13, D-81377 Munich, Germany, and Arrhenius Laboratory, Department of Organic Chemistry, Stockholm University, SE-10691 Stockholm, Sweden

Received February 1, 2002

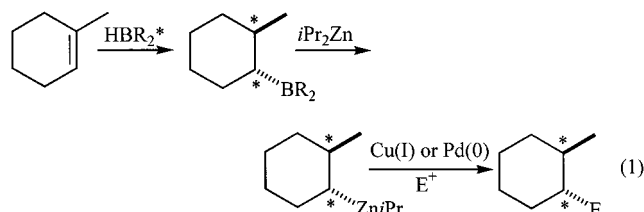
The mechanism of the boron–zinc exchange reaction has been studied by applying density functional calculations at the B3PW91 level of theory. It was found that the exchange reaction proceeds with a low activation barrier, involving two intermediates with unusual bonding structures. The metal–carbon bonding in these intermediates ensures a highly stereoselective exchange process, which can be employed in asymmetric organometallic synthesis. On the basis of the theoretical results we predict that organogallium and organoindium compounds can also be generated by alkyl exchange reactions from organoboranes.

## I. Introduction

Chiral organometallic species are very useful synthetic intermediates, because of their potential to undergo highly stereo- and enantioselective reactions with electrophiles. To obtain high enantioselectivity in these reactions, the chiral organometallic species have to comply with three important requirements: (1) the enantiomerically enriched organometallic reagent should be readily accessible through a stereo- or enantioselective reaction, (2) the inversion barrier of the metalated carbon must be sufficiently high to ensure that the organometallic compound is configurationally stable under the reaction conditions, and (3) reaction with electrophiles must occur with very high stereoselectivity. Knochel and co-workers have demonstrated that secondary organozinc compounds mainly satisfy the above requirements.<sup>1</sup>

The synthetic utility of chiral organozinc reagents arises from the fact that these organometallic species can be easily generated from optically active organoboranes, which are in turn available via asymmetric hydroboration using, for example, mono(isopinocampheyl)borane<sup>2</sup> ((-)-IpcBH<sub>2</sub>). It has been shown that the chiral alkyl group of an organoborane can easily be exchanged in a highly stereoselective process with an alkyl group of a simple dialkylzinc reagent to provide a chiral organozinc species.<sup>1a</sup> Furthermore, the boron–zinc exchange proceeds with clear retention of the configuration of the stereogenic carbon.<sup>1c</sup> Subse-

quently, the chiral organozinc compound can be reacted, for example, in copper(I)-mediated<sup>1d</sup> or palladium(0)-catalyzed<sup>1e</sup> reactions, with a broad range of electrophiles (E<sup>+</sup>), to give the desired products in high enantiomeric excess (eq 1). A synthetically important aspect of the



above methodology is that the chiral products can be obtained from functionalized alkenes in a one-pot sequence.

The broad synthetic scope of the above asymmetric process relies on the fact that the boron–zinc exchange takes place with ease and with high stereoselectivity. Although the boron–zinc exchange process is known from the literature,<sup>3</sup> many important mechanistic details, such as the structure and stability of the reaction intermediates and the source of the excellent stereoselectivity, have remained unstudied. In this study we present computational results obtained for the description of the potential energy surface of the methyl group exchange between trimethylborane and dimethylzinc (Figures 1 and 2) and for the analysis of the unique bonding structure of the reaction intermediates (Figures 3 and 4). In addition, we have studied the potential for alkyl exchange reactions between trimethylborane and methylated magnesium, aluminum, gallium, and indium organometallics (Figures 1 and 5).

(3) (a) Thiele, K. H.; Engelhardt, G.; Köhler, J.; Arnstedt, M. *J. Organomet. Chem.* **1967**, *9*, 385. (b) Oppolzer, W.; Radinov, R. N. *Helv. Chem. Acta* **1992**, *75*, 170. (c) Srebnik, M. *Tetrahedron Lett.* **1991**, *32*, 2449. (d) Agrios, K. A.; Srebnik, M. *J. Org. Chem.* **1994**, *59*, 5468.

\* To whom correspondence should be addressed. E-mail: kalman@organ.su.se.

<sup>†</sup> Ludwig-Maximilians-University Munich.

<sup>‡</sup> Stockholm University.

(1) (a) Boudier, A.; Darcel, C.; Flachsman, F.; Micouin, L.; Oestreich, M.; Knochel, P. *Chem. Eur. J.* **2000**, *6*, 2748. (b) Boudier, A.; Hupe, E.; Knochel, P. *Angew. Chem., Int. Ed.* **2000**, *39*, 2294. (c) Hupe, E.; Knochel, P. *Org. Lett.* **2001**, *3*, 127. (d) Boudier, A.; Flachsman, F.; Knochel, P. *Synlett* **1998**, 1438. (e) Boudier, A.; Knochel, P. *Tetrahedron Lett.* **1999**, *40*, 687.

(2) Brown, H. C.; Mandal, A. K.; Yoon, N. M.; Singaram, B.; Schwier, J. R.; Jadhav, P. K. *J. Org. Chem.* **1982**, *47*, 5069.

## II. Results and Discussion

**Computational Methods.** Unless otherwise stated, all geometries were fully optimized employing the Becke-type<sup>4a</sup> three-parameter density functional model B3PW91, using the Gaussian98 program package.<sup>5</sup> This so-called hybrid functional includes the exact (Hartree–Fock) exchange, the gradient-corrected exchange functional of Becke,<sup>4a</sup> and the more recent correlation functional of Perdew and Wang.<sup>4b</sup> The geometry optimizations for the species **1–4** were carried out with Pople's 6-31G\*<sup>4c–1</sup> basis set. The calculations for **5a–c** have been carried out using the SDD(d) basis set, including the D95V(d) basis<sup>4j</sup> on carbon, hydrogen, and boron, as well as the Stuttgart/Dresden<sup>4k,1</sup> pseudopotentials and basis augmented with a d polarization function<sup>4m</sup> (exponent 0.16) on indium.

Harmonic frequencies were calculated at the level of optimization for **1–5** to characterize the calculated stationary points and to determine the zero-point energies (ZPE). The fully optimized transition-state structures **1b,d**, **3b**, **4b**, and **5b** were characterized by a single imaginary frequency, while the rest of the fully optimized structures possess only real frequencies.

To characterize the metal–carbon bonding in intermediates **1c,e**, the B3PW91/6-31G\*\*//B3PW91/6-31G\* electron densities were analyzed by the “atoms in molecule” (AIM) method of Bader and co-workers<sup>6a</sup> using the AIM2000 program package.<sup>6b</sup>

**Potential Energy Surface of the B–Zn Exchange.** We studied the methyl exchange between BMe<sub>3</sub> and ZnMe<sub>2</sub> as a model reaction to understand the synthetically important B–Zn exchange processes. Thus, the substrates and final products of the exchange reaction studied are identical and the potential energy surface is symmetrical (Figure 2). The two substrate molecules form a weakly bonded electrostatic complex (**1a**) in which the boron–zinc separation is relatively

large (2.854 Å, Figure 1). The electrostatic interaction has a very weak effect on the Zn–C bonding in ZnMe<sub>2</sub>. As the two monomers approach each other, a four-membered-ring adduct (**1c**) is formed, which has C<sub>s</sub> symmetry. In this interesting intermediate, the boron atom, the zinc atom, and the ring carbons are all hypervalent (vide infra). The B–C bond in the ring (1.791 Å) is much longer than the endocyclic B–C bonds (1.616 Å). Similarly, the exocyclic Zn–C bond (2.092 Å) is longer than the endocyclic one. Formation of intermediate **1c** from **1a** occurs via the transition state (TS) structure **1b**, requiring a low activation energy of 6.6 kcal mol<sup>-1</sup>. Intermediate **1c** may undergo two different processes. Recovery of the starting materials (**1a**) proceeds through a very low activation barrier (0.6 kcal mol<sup>-1</sup>). Alternatively, **1c** can be transformed into another intermediate, **1e**, passing through TS **1d**, which also requires only 0.6 kcal mol<sup>-1</sup> activation energy. Intermediate **1e** has C<sub>3v</sub> symmetry and a unique bonding structure, including a direct boron–zinc bond. In this adduct the equatorial C–B bonds (1.710 Å) are longer than the axial C–B bond (1.614 Å), and the distance between the equatorial carbons and Zn (2.275 Å) is much longer than the axial Zn–C bond (1.926 Å). Adduct **1e** is more stable (by 1.6 kcal mol<sup>-1</sup>) than the four-membered-ring intermediate **1c**. In the case of methyl group exchange the separated monomers can be obtained by repeating the **1e** → **1d** → **1c** → **1b** → **1a** sequence.

**Bonding Structure of Adducts 1c,e.** Analysis of the electron density distribution ( $\rho(\mathbf{r})$ ) resulted in four (3, -1) bond critical points ( $\mathbf{r}_b$ ) and one (3, 1) ring critical point for the B–Me–Zn–Me four-membered-ring fragment of **1c** (Figure 3). The energy density ( $H(\mathbf{r}_b)$ ) is negative in all four bond critical points, indicating a covalent character.<sup>6c</sup> The exocyclic B–Me and Zn–Me bonds can also be characterized as covalent bonds. Thus, in this interesting complex both the B and Zn atoms have a hypervalent character. The electron density in the bond critical points of the exocyclic metal–carbon bonds is lower than that of the endocyclic ones, indicating a weaker metal–carbon bonding in the four-membered-ring fragment. The bonding structure of intermediate **1e** is also very interesting. A bond critical point was found through the B–Zn internuclear axis, indicating a covalent B–Zn single bond. In addition, the AIM analysis indicates four B–C covalent bonds in **1e**, suggesting that the boron atom is pentacoordinated in this adduct. Although there are no bond critical points between the zinc and the carbon atoms attached to boron, the relatively short C(B)–Zn distance (2.275 Å) and the unusually wide H–C–B angle (128.2°) clearly indicate a strong interaction between the equatorial methyl groups and zinc.

Analysis of the MO's in **1e** indicates that the B–Zn bond is composed of three high-lying MO's, including the HOMO (Figure 4). The major contribution to the B–Zn bonding orbitals arises from the s–p orbitals of boron and zinc; however, the admixture of the 3d AO's of Zn is also significant.

The hypervalency of the ring carbons in **1c** and the strong C(B)–Zn interaction in **1e** have important implications for the stereochemistry of the B–Zn exchange reaction. In both intermediates the carbons undergoing exchange have a front-side interaction with the boron

(4) (a) Becke, A. D. *J. Chem. Phys.* **1993**, *98*, 5648. (b) Perdew, J. P.; Wang, Y. *Phys. Rev. B* **1992**, *45*, 13244. (c) Ditchfield, R.; Hehre, W. J.; Pople, J. A. *J. Chem. Phys.* **1971**, *54*, 724. (d) Hehre, W. J.; Ditchfield, R.; Pople, J. A. *J. Chem. Phys.* **1972**, *56*, 2257. (e) Hariharan, P. C.; Pople, J. A. *Mol. Phys.* **1974**, *27*, 209. (f) Gordon, M. S. *Chem. Phys. Lett.* **1980**, *76*, 163. (g) Hariharan, P. C.; Pople, J. A. *Theor. Chim. Acta* **1973**, *28*, 213. (h) Francl, M. M.; Pietro, W. J.; Hehre, W. J.; Binkley, J. S.; Gordon, M. S.; DeFrees, D. J.; Pople, J. A. *J. Chem. Phys.* **1982**, *77*, 3654. (i) Rasslov, V. A.; Pople, J. A.; Ratner, M. A.; Windus, T. L. *J. Chem. Phys.* **1998**, *109*, 1223. (j) Dunning, T. H.; Hay, P. J. In *Modern Theoretical Chemistry*; Schaefer, H. F., III, Ed.; Plenum: New York, 1977; Vol. 3.1. (k) Bergner, A.; Dolg, M.; Kuechle, W.; Stoll, H.; Preuss, H. *Mol. Phys.* **1993**, *80*, 1431. (l) Leininger, T.; Berning, A.; Nicklass, A.; Stoll, H.; Werner, H.-J.; Flad, H.-J. *Chem. Phys.* **1997**, *217*, 19. (m) Huzinaga, S.; Andzelm, J.; Klobukowski, K.; Radzio-Adzelm, E.; Sakai, Y.; Tatewaki, H. *Gaussian Basis Sets for Molecular Calculations*; Elsevier: Amsterdam, 1984.

(5) Frisch, M. J.; Trucks, G. W.; Schlegel, H. B.; Scuseria, G. E.; Robb, M. A.; Cheeseman, J. R.; Zakrzewski, V. G.; Montgomery, J. A., Jr.; Stratmann, R. E.; Burant, J. C.; Dapprich, S.; Millam, J. M.; Daniels, A. D.; Kudin, K. N.; Strain, M. C.; Farkas, O.; Tomasi, J.; Barone, V.; Cossi, M.; Cammi, R.; Mennucci, B.; Pomelli, C.; Adamo, C.; Clifford, S.; Ochterski, J.; Petersson, G. A.; Ayala, P. Y.; Cui, Q.; Morokuma, K.; Malick, D. K.; Rabuck, A. D.; Raghavachari, K.; Foresman, J. B.; Cioslowski, J.; Ortiz, J. V.; Stefanov, B. B.; Liu, G.; Liashenko, A.; Piskorz, P.; Komaromi, I.; Gomperts, R.; Martin, R. L.; Fox, D. J.; Keith, T.; Al-Laham, M. A.; Peng, C. Y.; Nanayakkara, A.; Gonzalez, C.; Challacombe, M.; Gill, P. M. W.; Johnson, B. G.; Chen, W.; Wong, M. W.; Andres, J. L.; Head-Gordon, M.; Replogle, E. S.; Pople, J. A. *Gaussian 98*, revisions A.3 and A.7; Gaussian, Inc.: Pittsburgh, PA, 1998.

(6) (a) Bader, R. F. W. *Atoms in Molecules: A Quantum Theory*; Clarendon Press: Oxford, U.K., 1990. (b) Biegler-König, F.; Schönbohm, J.; Bayles, D. *J. Comput. Chem.* **2001**, *22*, 545. (c) Kraka, K.; Cremer, D. In *The Concept of the Chemical Bond*; Maksic, Z. B., Ed.; Springer: Berlin, 1990; p 453.

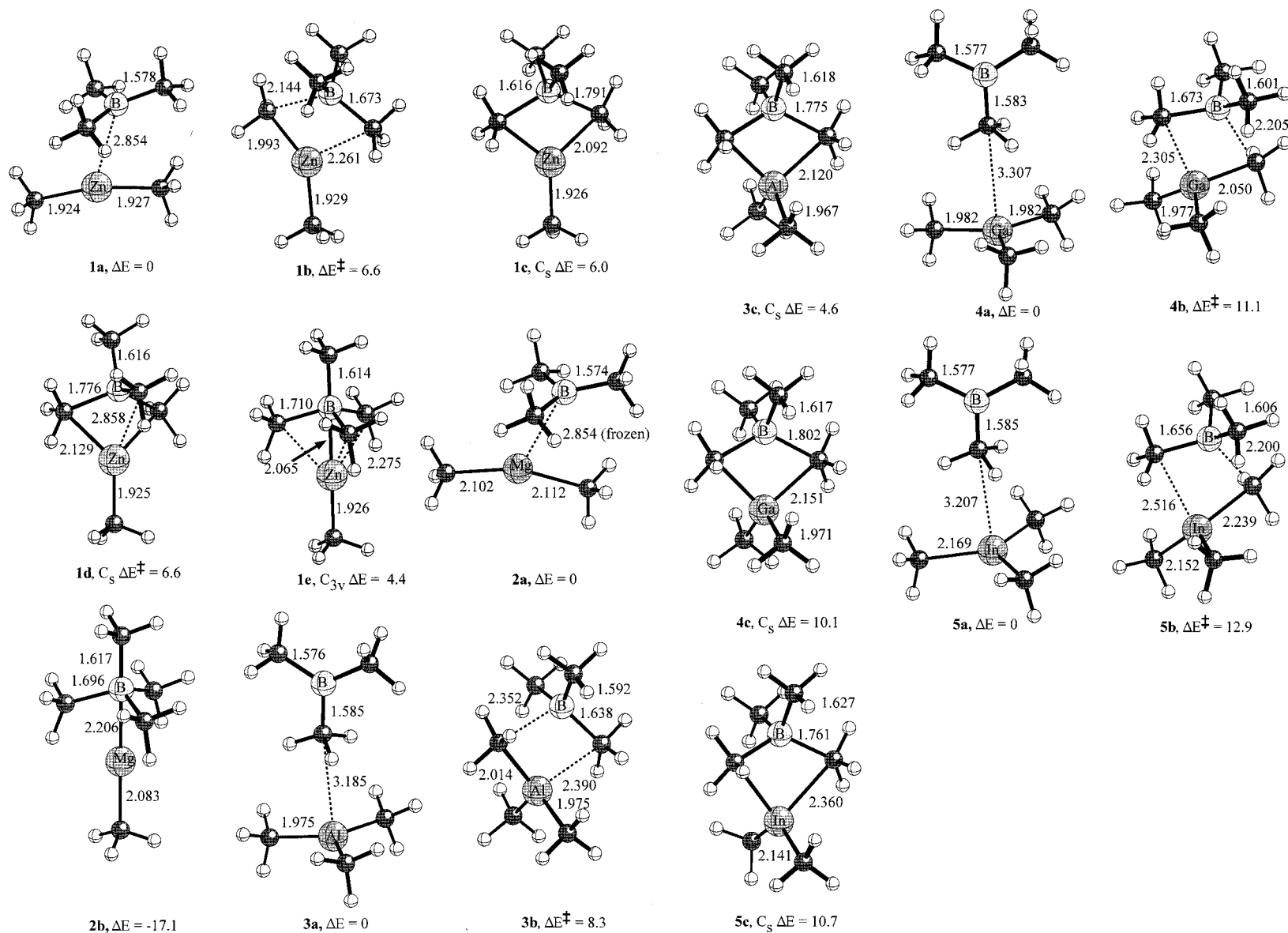


**Figure 1.** B3PW91 geometries and energies of the methyl exchange processes. Except for the relative energy of **2b**, the energies are ZPE-corrected. All energy values are given in kcal mol<sup>-1</sup>. All geometries are fully optimized with the B3PW91 functional (bond lengths in Å). The exception is **2a**, in which the Mg–B distance is restricted, while the rest of the parameters are fully optimized.

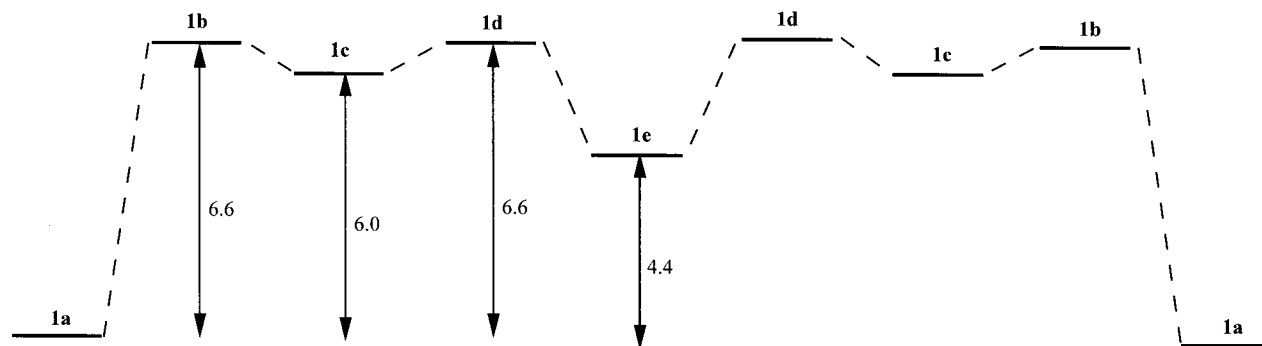


**Figure 2.** Reaction profile for the boron–zinc exchange process. All the energies are ZPE-corrected and given in kcal mol<sup>-1</sup>.

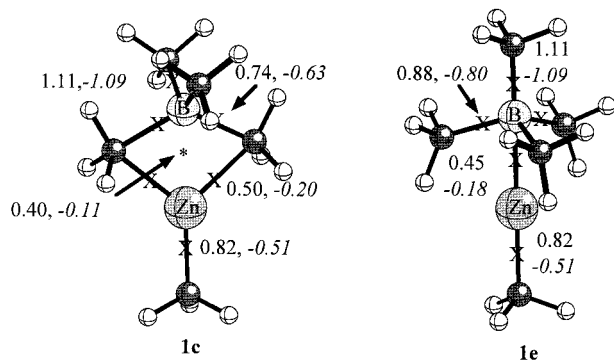


**Figure 3.** Selected critical points obtained by the AIM analysis for **1c,e** (X denotes bond critical points, and the asterisk denotes the ring critical point) with the value of the electron density  $\rho(\mathbf{r})$  (e Å<sup>-3</sup>) and the energy density  $H(\mathbf{r})$  (hartree Å<sup>-3</sup>) (in italics) at the corresponding critical points.

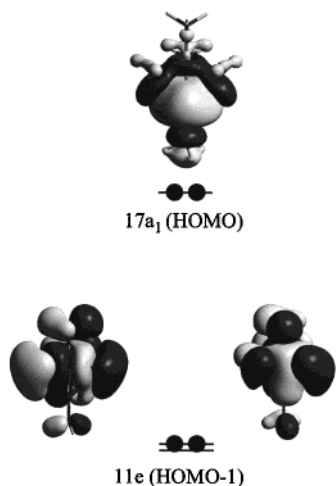


**Figure 4.** Boron–zinc bonding MO's in adduct **1e**.

and zinc atoms. This front-side interaction preserves the configuration of the asymmetric carbons in the exchange process, resulting in the retention of chirality. In addition, the hypervalency of boron and zinc in **1c,e** prevents an external addition of a chiral carbon to one of the metal centers, and thus S<sub>N</sub>2-type processes involving inversion of configuration can be avoided.

Another important structural feature of **1c** and **1e** is the tetrahedral configuration of the methyl groups on boron with a relatively short B–C bond length (1.61–1.79 Å). This also means that bulky alkyl groups, such as chiral alkyl functionalities, will preferentially reside on zinc instead of boron. Thus, bulky chiral groups

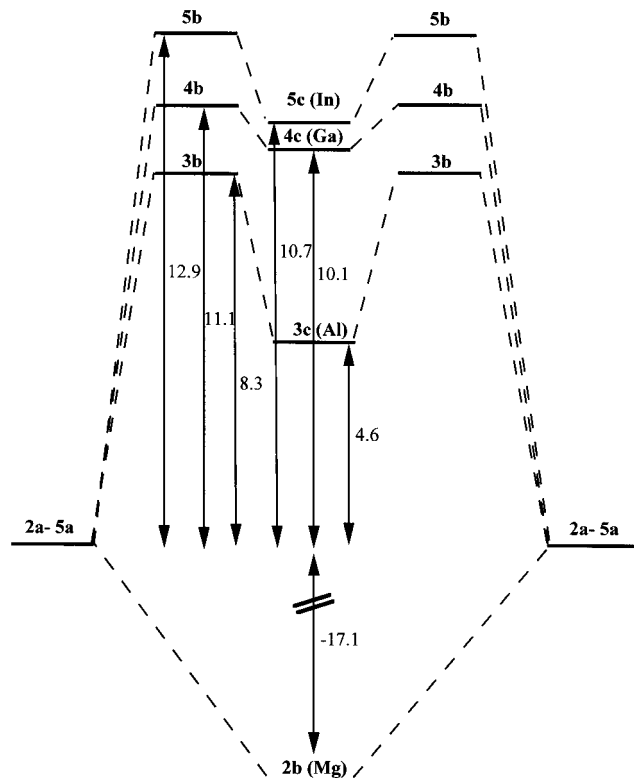


**Figure 5.** Reaction profiles for B–M (M = Mg, Al, Ga, In) exchange processes. All energies are given in kcal mol<sup>-1</sup>.

formed in the hydroboration reaction can be transferred efficiently to the zinc atom under the reaction conditions of the B–Zn exchange process.<sup>1</sup>

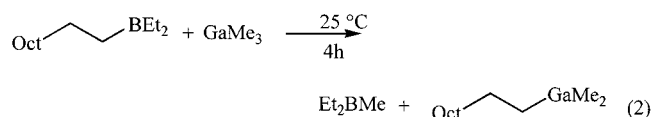
**Extension to Other Boron–Metal Exchange Reactions.** Understanding of the mechanism of the B–Zn exchange raises the question of the possibility of performing alkyl exchange reactions between boron and other metals to form new synthetically interesting organometallic reagents. Accordingly, we considered replacing the Zn–alkyl reagents with Mg–, Al–, Ga–, and In–alkyls.

The DFT calculations show (Figures 1 and 5) that the covalent magnesium–boron adduct **2b** (similar to the boron–zinc adduct **1e**) is particularly stable. It was found that the weakly bonded adduct of Mg(CH<sub>3</sub>)<sub>2</sub> and B(CH<sub>3</sub>)<sub>3</sub>, corresponding to **1a**, does not represent a minimum on the potential energy surface, but these species form adduct **2b** without an activation barrier. In order to compare the energetics of the **1a** → **1e** process to the corresponding process involving magne-

sium, the magnesium–boron distance in **2a** was frozen in the geometry optimization procedure. It was found that adduct **2b** is more stable by 17.1 kcal mol<sup>-1</sup> than the weakly bound complex of the separated species (**2a**). This also shows that methyl exchange between Mg(CH<sub>3</sub>)<sub>2</sub> and B(CH<sub>3</sub>)<sub>3</sub> cannot be accomplished, because the alkylated reactants cannot be separated.

The weakly bound complex of Al(CH<sub>3</sub>)<sub>3</sub> and B(CH<sub>3</sub>)<sub>3</sub>, **3a**, represents a minimum on the potential energy surface. In this complex the two monomers held together by van der Waals forces are separated by 3.2 Å. Formation of the intermediate of the methyl exchange (**3c**) proceeds through a low activation barrier of 8.3 kcal mol<sup>-1</sup> (**3b**). Adduct **3c** (similar to **1c**) is remarkably stable (4.6 kcal mol<sup>-1</sup>) compared to the separated reactants. This means that the alkyl exchange between boron and aluminum may be unfeasible because of the high stability of adduct **3c**. This is in agreement with the work of Köster and Bruno,<sup>7</sup> who showed that a possible alkyl exchange from B to Al very much depends on the ability to form stable associates.

Replacement of Al with Ga or In leads to the weakly bonded complexes **4a** and **5a**, in which the monomers are separated by 3.2–3.3 Å. These weakly bonded complexes are much more stable than the corresponding four-membered-ring adducts (**4c** and **5c**). The structures of adducts **4c** and **5c** are very similar to that of intermediate **1c** of the B–Zn exchange; however, formation of **4c** and **5c** involves a much higher activation barrier than the corresponding process in the B–Zn exchange reaction. These theoretical results suggest that chiral Ga and In compounds could be generated from organoboranes by an exchange reaction. Indeed, according to our preliminary experimental studies, an alkyl exchange reaction of diethyldecylborane with trimethylgallium proceeds smoothly at room temperature to yield dimethyldecylgallium (ca. 85% conversion, eq 2).



Further evidence for such an alkyl exchange process from B to Ga was obtained by NMR studies. A 1:1 mixture of trimethylgallium and triethylborane clearly showed the formation of at least one new trialkylborane and one new trialkylgallium species.<sup>8</sup>

### III. Conclusions

We have shown that the B–Zn exchange proceeds with a low activation energy and involves intermediates

(7) (a) Köster, R.; Bruno, G. *Liebigs Ann. Chem.* **1960**, 629, 89. (b) Köster, R. *Angew. Chem.* **1959**, 71, 520.

**1c,e**. The carbon–metal bonding structure of the reaction intermediates ensures clean retention of the configuration of the alkyl group which is exchanged. Exchange of zinc with magnesium leads to a stable adduct (**2b**) which hinders the alkyl exchange between the monomers. Comparison of the reaction profiles for the methyl exchange of B(CH<sub>3</sub>)<sub>3</sub> with Al(CH<sub>3</sub>)<sub>3</sub>, Ga(CH<sub>3</sub>)<sub>3</sub>, and In(CH<sub>3</sub>)<sub>3</sub> reveals a clear trend. As one goes from aluminum to indium, the activation barrier increases and the stability of the reaction intermediate (**3c–5c**) decreases. On the basis of these theoretical results and our preliminary experimental results, we conclude that synthetically useful gallium and indium organometallics can probably be generated via exchange reactions using organoboranes.

## IV. Experimental Section

**Synthesis of Dimethyldecylgallium and Iodolysis.** A flame-dried 25 mL flask equipped with a magnetic stirring bar, an argon inlet, and a septum was charged with decene (140 mg, 1 mmol). Et<sub>2</sub>BH (0.4 mL, 7.3 M in Me<sub>2</sub>S, 3 equiv) was added, and the resulting mixture was stirred for 16 h at 50 °C. After the volatiles were pumped off (0.1 mmHg, 25 °C, 2 h), GaMe<sub>3</sub> (0.32 mL, 3 mmol, 3 equiv) was added, and the mixture was stirred for 4 h at 25 °C. The decyl transfer from boron to gallium was ca. 85%, as monitored by GC analysis of oxidized aliquots (aqueous 3 M NaOH/aqueous 30% H<sub>2</sub>O<sub>2</sub>). The volatiles were pumped off (0.1 mmHg, 25 °C, 0.5 h), and THF (2 mL) was added. After the mixture was cooled to 0 °C, a solution of I<sub>2</sub> (1.52 g, 6 mmol, 6 equiv) in THF (2 mL) was added dropwise over 30 min. The mixture was stirred for 30 min at 25 °C. GC analysis of the reaction mixture after treatment with Na<sub>2</sub>S<sub>2</sub>O<sub>3</sub>(aq) and extraction with Et<sub>2</sub>O showed the formation of MeI and DecI in an approximate 2:1 ratio.

**Acknowledgment.** This work was supported by the Swedish Research Council (VR) and the Deutsche Forschungsgemeinschaft (Leibniz-Program). E.H. thanks the Fonds der Chemischen Industrie for a Kekulé fellowship. The calculations were done at the IBM SP2 parallel computer facility of the Paralleldatorzentrum (PDC) at the Royal Institute of Technology of Sweden. We thank the PDC for a generous allotment of computer time.

**Supporting Information Available:** Tables giving Cartesian coordinates of adducts **1–5**. This material is available free of charge via the Internet at <http://pubs.acs.org>.

OM020083N

(8) The typical B–CH<sub>2</sub> coupling pattern shows clearly the existence of at least two different B–CH<sub>2</sub>CH<sub>3</sub> groups in the <sup>13</sup>C NMR. Furthermore, the <sup>11</sup>B NMR spectrum consists of two peaks with a chemical shift that is typical for trialkylboranes. An APT experiment shows the existence of a singlet for a –CH<sub>2</sub>– group that can thus only be a –CH<sub>2</sub>–CH<sub>3</sub> group attached to gallium.